reflections, numerical absorption correction (min./max. transmission: 0.546/0.664), 256 parameters. $R_1 = 0.042$, $wR_2 = 0.122$ (all data), max. residual electron density 0.64 e Å^{-3}. In the refinement a merohedral twinning from 6/*m* into 6/*mmm* with volume fractions of 91:9 was considered. One THF molecule of the $[Li(thf)_4]^+$ ion is disordered over a C_3 axis. Crystallographic data (excluding structure factors) for the structures reported in this paper have been deposited with the Cambridge Crystallographic Data Centre as supplementary publication no. CCDC-101051. Copies of the data can be obtained free of charge on application to CCDC, 12 Union Road, Cambridge CB21EZ, UK (fax: (+44) 1223-336-033; e-mail: deposit@ccdc.cam.ac.uk).

[13] G. Linti, W. Köstler, A. Rodig, *Eur. J. Inorg. Chem.* **1998,** *745*, 749.
[14] G. Linti, W. Köstler, *Chem. Eur. J.* **1998**, *4*, 942 – 949.
[15] RI-DFT calculations with program package TURBOMOLE. All distances were multiplied by 0.97 to fit with experimental data of **1**: R. Ahlrichs, Universität Karlsruhe; K.Eichkorn, O. Treutler, H. Öhm, M. Häser, R. Ahlrichs, *Chem. Phys. Lett.* **1995**, *240*, 283.
[16] a) E. R. Davidson, *J. Chem. Phys.* **1967**, *46*, 3320; b) K. R. Roby, *Molec. Phys.* **1974**, *27*, 81; c) R. Heinzmann, R. Ahlrichs, *Theoret. Chim. Acta* **1976**, *42*, 33.
[17] P. von R. Schleyer, G. Subramanian, A. Dransfeld, *J. Am. Chem. Soc.* **1996**,*118*, 9988 – 9989.
[18] a) $[As_2(AlCp^*)_3]$: C. K. F. von Hänisch, C. Üffing, M. A. Junker, A. Ecker, B. O. Kneisel, H. Schnöckel, *Angew. Chem.* **1996**, *108*, 3003 – 3005; *Angew. Chem. Int. Ed. Engl.* **1996**, *35*, 2875 – 2877; b) $Et_5B_3C_2$: M. Antipin, R. Boese, D. Bläser, A. Maulitz, *J. Am. Chem. Soc.* **1997**, *119*, 326 – 333; c) $[(Me_3Si)_3CIn]_4S$: W. Uhl, R. Graupner, W. Hiller, M. Neumayer, *Angew. Chem.* **1997**, *109*, 62 – 64; *Angew. Chem. Int. Ed. Engl.* **1997**, *36*, 62 – 64.
[19] a) H. Gilman, C. L. Smith, *J. Organomet. Chem.* **1968**, *14*, 91; b) G. Gutekunst, A. G. Brook, *ibid.* **1982**, *225*, 1; c) A. Heine, R. Herbst-Irmer, G. M. Sheldrick, D. Stalke, *Inorg. Chem.* **1993**, *32*, 2694 – 2698.

Olefin Epoxidation by Methyltrioxorhenium: A Density Functional Study on Energetics and Mechanisms**

Philip Gisdakis, Serge Antonczak, Sibylle Köstlmeier, Wolfgang A. Herrmann, and Notker Rösch*

Oxygen transfer reactions mediated by transition metals, such as olefin epoxidation[1] and dihydroxylation,[2] are currently attracting much interest from both experimentalists and theoreticians. Many investigations, several of them of computational thrust, have unraveled details of olefin dihydroxylation as catalyzed by oxo complexes of the type MO_4 (M = Os, Ru).[3] Extensive experimental work has been devoted to the structurally similar compound methyltrioxorhenium (MTO) which has proven to be a highly efficient olefin epoxidation catalyst in the presence of hydrogen peroxide.[4] MTO reacts with H_2O_2 resulting in mono- and bisperoxo compounds; an additional aquo ligand has been found to stabilize the latter complex.[5] Recent experimental work shows the possibility for olefin epoxidation also by inorganic compounds like ReO_4^-, even without explicit use of H_2O_2.[6] Herrmann et al.[5] and Espenson et al.[7] have proposed reaction mechanisms for epoxidation by MTO-related complexes that involve differently oxygenated and hydrated forms of these catalysts. Also conceivable are processes in which hydroperoxo species participate.[8] However, in contrast to dihydroxylation by oxo complexes,[3] quite a few details of the reaction mechanism involving peroxo complexes remain to be clarified. Previous computational studies focused on structural aspects of MTO-related oxo complexes.[9] Here, we use density functional (DF) calculations[10, 11] to analyze structural and energetic properties of various mono-, bis-, and hydroperoxo derivatives of MTO and to estimate the activation barriers of the corresponding oxygen-transfer reactions.

We start by considering various rhenium – oxo and -peroxo complexes: MTO (**1**) as well as the corresponding monoperoxo (**2**) and bisperoxo (**3**) complexes, each of them in free (**A**) and monohydrated (**B**) form (Figure 1). The water ligand of complexes **B** was added in *cis* position to the methyl group, as suggested by an X-ray structure analysis for the bisperoxo complex.[5] A second water molecule in *trans* position is

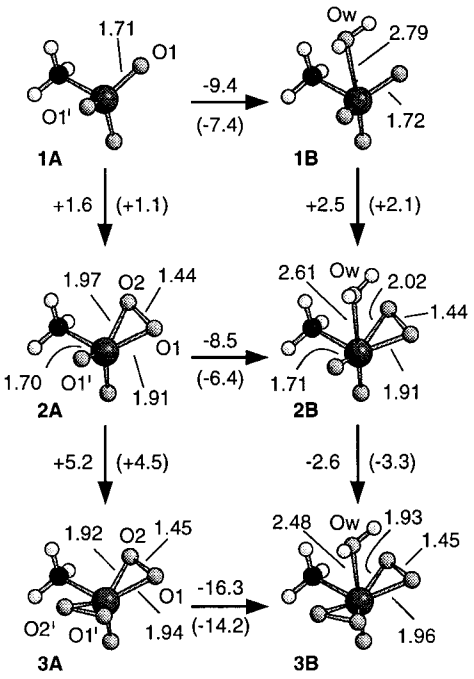

Figure 1. Optimized structures of **1A** and the corresponding monoperoxo (**2A**) and bisperoxo complexes (**3A**) as well as the mono-hydrated complexes **1B**, **2B**, and **3B**. Bond lengths in Å, energy and enthalpy (in parentheses) changes of peroxidation (columns) and hydration (rows) in kcal mol^{-1}. Experimental bond lengths for **3B**:[5] Re – O1 1.91, Re – O2 1.90, O1 – O2 1.47, Re – Ow 2.25.

[*] Prof. Dr. N. Rösch, Dipl.-Chem. P. Gisdakis, Dr. S. Antonczak, Dr. S. Köstlmeier
Lehrstuhl für Theoretische Chemie
der Technischen Universität München
D-85747 Garching (Germany)
Fax: (+49) 89-289-13622
E-mail: roesch@theochem.tu-muenchen.de
Prof. Dr. W. A. Herrmann
Anorganisch-chemisches Institut der Technischen Universität München (Germany)

[**] This work was supported by the Deutsche Forschungsgemeinschaft, Bayerischer Forschungsverbund Katalyse (FORKAT), the German Bundesministerium für Bildung, Wissenschaft, Forschung und Technologie (no. 03D0050B), and the Fonds der Chemischen Industrie.

calculated to be weaker bound in the pertinent complexes of **2** and **3** (not shown in Figure 1). Furthermore, a water ligand in **1** in *trans* position has a slightly shorter bond length to the metal center, but essentially the same binding energy as one in *cis* position. To facilitate comparison, we discuss in the following only model structures with the aquo ligand in *cis* position. As expected for a Re center with strong Lewis acidity,[16] hydration leads to significant stabilization, yielding an important contribution to the energy of MTO peroxidation (Figure 1). The hydration energies for MTO **1A** and the monoperoxo complex **2A** are similar and much closer to each other than that of the bisperoxo complex **3A**, which is especially large (-16.3 kcal mol^{-1}). This latter finding underlines the particular stability of complex **3B** for which an X-ray structure is available.[5] Agreement between calculated and experimental[5] geometries of **3B** is very satisfactory; the bond length deviations are, in general, at most 0.04 Å. The Re–Ow bond length is an exception (exp. 2.25 Å,[5] calc. 2.48 Å); this deviation can be rationalized by a co-crystallized ether molecule.[5] If this crystal environment effect is modeled by two dimethyl ether molecules that form hydrogen bonds with the coordinated water, the calculated value of the Re–Ow bond length reduces to 2.34 Å (exp. 2.25 Å[5]). The peroxo groups are asymmetrically bound to the rhenium center; the tilting of the peroxo ligands relative to the "front" and "back" side (that is, the side that is furthest from and nearest to the methyl ligand, respectively) is different in complexes **2** and **3** (cf. bond lengths Re–O1 and Re–O2, Figure 1).

MTO is catalytically active in the presence of H_2O_2.[5, 7] Therefore, we studied olefin epoxidation by the unsolvated (**2A**, **3A**) and monosolvated peroxo complexes (**2B** and **3B**), and characterized transition states[17] for various mechanisms (Figure 2). Direct oxygen transfer to the olefin, in spiro fashion,[18] as all located transition states showed (see below), may occur when the olefin double bond directly attacks the peroxo group O1–O2 either from the front (O1, "spiro", **S**) or back (O2, "back-spiro", **BS**). Insertion (**I**) via a [2 + 2]-like arrangement[19] leads to a five-membered ring intermediate involving the metal center and a peroxo ligand (Figure 2); the epoxide is extruded from the complex via a second transition state (not discussed subsequently because the corresponding first step is energetically unfavorable compared to the spiro processes). In the calculations no precoordination[19] of the olefin to the Re center was found for this reaction. Furthermore, we located five transition states[17] with spiro structures for attacks on the hydroperoxo derivative **4** (Scheme 1), which can be formally derived from **3B** by proton transfer from the aquo ligand to a peroxo group. With the OOH and OH groups stabilized by an interligand hydrogen bond, **4** is about 10 kcal mol^{-1} higher in energy than **3B**. An olefin attack at the β-O atom of the hydroperoxo group may be followed by proton transfer to three different groups (oxo, hydroxo, or peroxo, Scheme 1c). Attack at the α-O center may occur from either front or back (Scheme 1a, b), accompanied by the back transfer of the OH group to the Re center. Since the activation barriers of hydroperoxo processes are calculated to be rather high ($\Delta E^{\ddagger} = 29.8$ kcal mol^{-1} and higher, oxygen transfer to the olefin, Scheme 1a), we refrain from further discussing these transition states.

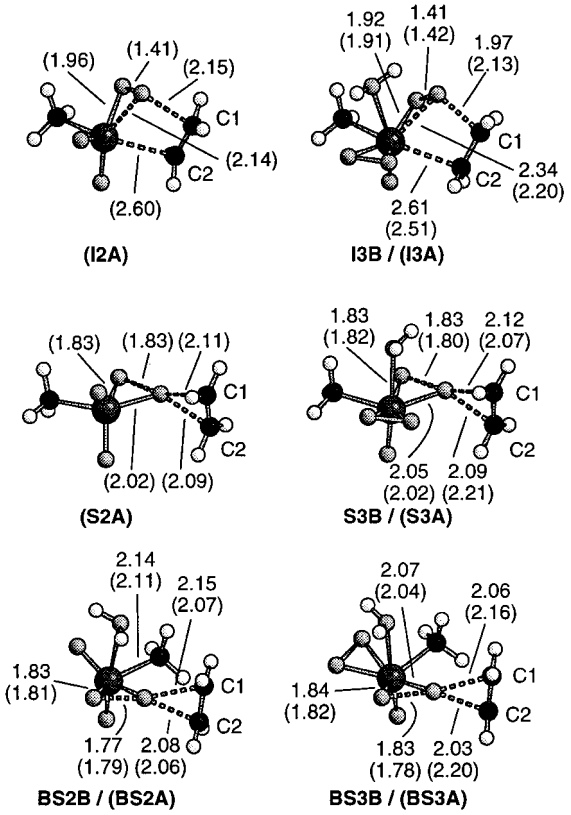

Figure 2. Various transition state structures for ethylene epoxidation by MTO-derived peroxo complexes (bond lengths in Å): spiro (**S**), back-spiro (**BS**), and insertion (**I**) processes involving complexes **2B** and **3B** (non-hydrated transition states **2A** and **3A** in parentheses).

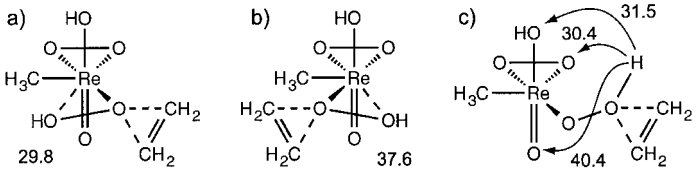

Scheme 1. Transition states for the ethylene epoxidation by the hydroperoxo complex **4** (in various conformations): attack of the α-O center from the "front" (a) and the "back" (b) as well as β-O approach (c) with subsequent H transfer to oxo, peroxo, or hydroxo ligands. Activation barriers (in kcal mol^{-1}) are given relative to complex **3B**.

In the following we will focus on oxygen transfer processes starting from the peroxo derivatives **2** and **3**; the calculated activation barriers $\Delta E^{\ddagger}$ and corresponding enthalpies $\Delta H^{\ddagger}_{298}$ for ethylene epoxidation are compared in Table 1. We shall identify these processes by their reaction type **S**, **BS**, or **I**

Table 1. Activation barriers $\Delta E^{\ddagger}$ and enthalpies $\Delta H^{\ddagger}_{298}$ (in parentheses) for the spiro (**S**), back-spiro (**BS**), and insertion (**I**) processes starting from complexes **2A**, **2B**, **3A**, and **3B** (see Figure 1). Energies given in kcal mol^{-1}.

	S	BS	I
2A	18.8 (18.5)	18.9 (18.8)	30.9 (31.7)
2B	–[a]	16.2 (16.6)	–[a]
3A	12.4 (13.0)	19.2 (19.6)	25.8 (26.6)
3B	16.2 (16.7)	23.3 (23.8)	38.7 (39.5)

[a] No transition state was localized since the water ligand is expelled during the search.

  1433-7851/98/3716-2212 $ 17.50+.50/0

combined with the metal complex involved, for example epoxidation via the spiro transition state with complex **3B** as catalyst is denoted as **S3B**. For complex **2B**, we were able to locate only transition state **BS2B** since the aquo ligand was expelled during the search for processes **S2B** and **I2B**.

In the transition states (Figure 2) the C–C olefin double bond is lengthened by 0.04 (**S**) to 0.07 Å (**I**). Compared to calculated transition states of organic epoxidation reactions,[20] the **S** and **BS** transition states feature an almost concerted approach of the olefin double bond to the active oxygen center where the attacked peroxo bond O1–O2 is significantly lengthened by about 0.4 Å, while the Re–O bond of the oxygen center to be transferred (**S**: O1, **BS**: O2) is elongated by about 0.1 Å only. The other Re–O bond of the attacked peroxo ligand shortens by the same amount on the way to a Re–O double bond. For process **S3B** (the one with the lowest activation barrier with respect to reactant **2A**), we verified that the reaction products are reached directly by following the transition vector.[21] During insertion the attacked Re–O bond is more elongated than in the mechanisms which proceed via spiro structures, while the corresponding O–O bond is somewhat contracted (Figure 2).

A comparison of the activation energies (Table 1) shows that for each complex insertion exhibits a noticeably higher barrier than either spiro approach. Comparing the two spiro approaches for each starting complex we note that for **3** a spiro attack from the front is clearly favored over a back-spiro process (by about 7 kcal mol^{-1}), while the opposite holds for **2**, even to the extent of aquo ligand extrusion in **S2B**. The water ligand in **2B** and **3B** enhances the barriers for all three types of mechanisms, with the exception of **BS2B** (cf. **BS2A**/**B**). This statement may be taken to include **S2B** and **I2B** where the transition states are essentially the same as in **S2A** and **I2A**, but the reactants are more stable due to water ligation. Apparently, two effects of hydration counteract each other to different degrees. While electron-donating and steric effects seem to dominate in **3** (although all metal–ligand bonds increase somewhat, compare **3A** and **3B**, Figure 1), the low barrier for **BS2B** correlates with a significant elongation of the attacked bond Re–O2 (by 0.05 Å, compare **2A** and **2B**). The transition state **S3A** has the lowest calculated barrier, but complex **3A** is significantly less stable than **3B** (by 16.3 kcal mol^{-1}, Figure 1). Thus, we conclude that epoxidation starting from **3** will proceed via transition state **S3B**. Compared to the measured activation enthalpy,[7] 10.2 ± 0.4 kcal mol^{-1}, for epoxidation of 4-methoxystyrene with a bisperoxo complex, the calculated energy barriers are of the same magnitude. The back-spiro process **BS2B** has essentially the same activation energy as **S3B**. Since the monoperoxo complex **2B** is only slightly less stable (by 2.6 kcal mol^{-1}) than the bisperoxo complex **3B**, processes **S3B** and **BS2B** are quite competitive.

Taking into account energies of hydration and peroxidation (Figure 1) as well as energies of activation (Table 1), one concludes that olefin epoxidation catalyzed by MTO/H_2O_2 occurs as direct oxygen transfer via transition states of spiro structure, likely involving both mono- and bisperoxo complexes depending on reaction conditions.[5, 7] Given the rather small differences among various lower lying transititon states, entropy effects (not included in the present study) may influence the selection among possible catalytically active complexes. Interaction of olefin substituents with the methyl ligand of the Re center along back-spiro pathways may further differentiate among the two spatial variants of attack (from front or back sides), and may thus influence the competition between mono- and bisperoxo starting complexes.

Received: January 23, 1998
Revised version: March 18, 1998 [Z 11395 IE]
German version: *Angew. Chem.* **1998**, *110*, 2333–2336

Keywords: density functional calculations · epoxidations · peroxo complexes · rhenium · transition states

[1] a) E. N. Jacobsen in *Catalytic Asymmetric Synthesis*, (Ed.: I. Ojima), VCH, New York, **1993**, p. 159; b) R. A. Sheldon, *Catalytic Oxidations with Hydrogen Peroxides as Oxidant*, Kluwer, Rotterdam, **1992**; c) K. A. Jorgensen, *Chem. Rev.* **1989**, *89*, 431.

[2] a) H. C. Kolb, M. S. VanNieuwenzhe, K. B. Sharpless, *Chem. Rev.* **1994**, *94*, 2483; b) R. A. Johnson, K. B. Sharpless, *Catalytic Asymmetry Synthesis*, VCH, Weinheim, **1993**.

[3] a) S. Dapprich, G. Ujaque, F. Maseras, A. Lledos, D. G. Musaev, K. Morokuma, *J. Am. Chem. Soc.* **1996**, *118*, 11660; b) U. Pidun, C. Boehme, G. Frenking, *Angew. Chem.* **1996**, *108*, 3008; *Angew. Chem. Int. Ed. Engl.* **1996**, *35*, 2817; c) D. W. Nelson, A. Gypser, P. T. Ho, H. C. Kolb, T. Kondo, H. Kwong, D. V. McGrath, A. E. Rubin, P. Norrby, K. P. Gable, K. B. Sharpless, *J. Am. Chem. Soc.* **1997**, *119*, 1840; d) M. Torrent, L. Deng, M. Duran, M. Sola, T. Ziegler, *Organometallics* **1997**, *16*, 13; e) E. J. Corey, M. C. Noe, *J. Am. Chem. Soc.* **1996**, *118*, 319.

[4] a) W. A. Herrmann, *J. Organomet. Chem.* **1995**, *500*, 149; b) W. A. Herrmann, F. E. Kühn, *Acc. Chem. Res.* **1997**, *30*, 169; c) C. C. Romão, F. E. Kühn, W. A. Herrmann, *Chem. Rev.* **1997**, *97*, 3197.

[5] W. A. Herrmann, R. W. Fischer, W. Scherer, M. U. Rauch, *Angew. Chem.* **1993**, *105*, 1209; *Angew. Chem. Int. Ed. Engl.* **1993**, *32*, 1157.

[6] A. K. Yudin, K. B. Sharpless, *J. Am. Chem. Soc.* **1997**, *119*, 11537.

[7] A. M. Al-Ajlouni, J. H. Espenson, *J. Am. Chem. Soc.* **1995**, *117*, 9243; A. M. Al-Ajlouni, J. H. Espenson, *J. Org. Chem.* **1996**, *61*, 3969.

[8] a) Y. Wu, D. K. W. Lai, *J. Org. Chem.* **1995**, *60*, 673; b) W. R. Thiel, *Chem. Ber.* **1996**, *129*, 575.

[9] a) T. Szyperski, P. Schwerdtfeger, *Angew. Chem.* **1989**, *101*, 1271; *Angew. Chem. Int. Ed. Engl.* **1989**, *28*, 1228; b) S. Köstlmeier, G. Pacchioni, W. A. Herrmann, N. Rösch, *J. Organomet. Chem.* **1996**, *514*, 111; c) S. Köstlmeier, O. D. Häberlen, N. Rösch, W. A. Herrmann, B. Solouki, H. Bock, *Organometallics* **1996**, *15*, 1872.

[10] Gaussian 94, Revision D.4, M. J. Frisch, G. W. Trucks, H. B. Schlegel, P. M. W. Gill, B. G. Johnson, M. A. Robb, J. R. Cheeseman, T. Keith, G. A. Petersson, J. A. Montgomery, K. Raghavachari, M. A. Al-Laham, V. G. Zakrzewski, J. V. Ortiz, J. B. Foresman, J. Cioslowski, B. B. Stefanov, A. Nanayakkara, M. Challacombe, C. Y. Peng, P. Y. Ayala, W. Chen, M. W. Wong, J. L. Andres, E. S. Replogle, R. Gomperts, R. L. Martin, D. J. Fox, J. S. Binkley, D. J. Defrees, J. Baker, J. P. Stewart, M. Head-Gordon, C. Gonzalez, J. A. Pople, Gaussian, Inc., Pittsburgh, PA, **1995**.

[11] The geometries of the complexes were optimized by using the B3LYP exchange correlation functional[12] with effective core potentials and double-ζ basis sets, LanL2DZ[13] on Re and 6–311G(d,p)[14] on H, C, and O, followed by single-point energy calculations, with a (441/2111/21/11) decontracted LanL2DZ basis set on Re[15] where two f-type exponents (0.5895 and 0.2683) were added on Re. For **3A**, **3B**, **S3B**, and **BS2A**, geometries were checked at the decontracted (441/2111/21) LanL2DZ level, yielding changes of bond lengths of less than 0.01 Å and of activation barriers of less than 0.2 kcal mol^{-1}. The enthalpy values (T = 298.15 K) were calculated by using unscaled vibrational frequencies obtained at the LanL2DZ level; the effect of

  1433-7851/98/3716-2213 $ 17.50+.50/0

this smaller basis set on the enthalpy correction terms was checked, and found to be less than 0.3 kcal mol^{-1}.
[12] a) A. D. Becke, J. Chem. Phys. **1993**, *98*, 5648; b) C. Lee, W. Yang, R. G. Parr, *Phys. Rev. B* **1988**, *37*, 785.
[13] a) T. H. Dunning, P. J. Hay in *Modern Theoretical Chemistry*, *Vol. 3* (Ed.: H. F. Schaefer III), New York, **1976**, p. 1; b) P. J. Hay, W. R. Wadt, *J. Chem. Phys.* **1985**, *82*, 299.
[14] a) R. Krishnan, J. Binkley, R. Seeger, J. Pople, *J. Chem. Phys.* **1980**, *72*, 650; b) A. McLean, G. Chandler, *J. Chem. Phys.* **1980**, *72*, 5639.
[15] G. Frenking, I. Antes, M. Böhme, S. Dapprich, A. W. Ehlers, V. Jonas, A. Neuhaus, M. Otto, R. Stegmann, A. Veldkamp, S. F. Vyboishchikov in *Reviews in Computational Chemistry*, *Vol. 8* (Eds.: K. B. Lipkowitz, D. B. Boyd), VCH, New York, **1996**, p. 63.
[16] S. Köstlmeier, V. A. Nasluzov, W. A. Herrmann, N. Rösch, *Organometallics* **1997**, *16*, 1786.
[17] All transition states were checked by a vibrational analysis at the LanL2DZ level.
[18] K. B. Sharpless, J. M. Townsend, D. R. Williams, *J. Am. Chem. Soc.* **1972**, *94*, 195.
[19] H. Mimoun, I. S. d. Roch, L. Sajus, *Tetrahedron* **1970**, *26*, 37.
[20] a) D. A. Singleton, S. R. Merrigan, J. Liu, K. N. Houk, *J. Am. Chem. Soc.* **1997**, *119*, 3385; b) R. D. Bach, C. M. Estévez, J. E. Winter, M. N. Glukhovtsev, *J. Am. Chem. Soc.* **1998**, *120*, 680.
[21] Internal reaction coordinate analysis carried out at the LanL2DZ level; see C. Gonzalez, H. B. Schlegel, *J. Chem. Phys.* **1990**, *94*, 5523.

The First Organically Templated Layered Uranium(IV) Fluorides: $(H_3N(CH_2)_3NH_3)U_2F_{10}\cdot 2H_2O$, $(H_3N(CH_2)_4NH_3)U_2F_{10}\cdot 3H_2O$, and $(H_3N(CH_2)_6NH_3)U_2F_{10}\cdot 2H_2O$**

Robin J. Francis, P. Shiv Halasyamani, and Dermot O'Hare*

Hydrothermal chemistry in the presence of organic structure-directing agents has been demonstrated to be a highly versatile technique for the synthesis of new layered and three-dimensional framework materials.[1, 2] The versatility of the technique derives from the exquisite control over the detailed topology of the inorganic framework that can be achieved by the systematic variation of the synthesis conditions and the template employed, and over recent years a vast range of novel open-framework and layered materials have been reported. All these materials contain the common structural feature of an inorganic anionic framework within which the cationic organic structure-directing agent is occluded. The continued interest in the synthesis of new materials in this class stems from their suitability for a range of materials chemistry applications including heterogenous catalysis,[3] molecular sieving, ion-exchange,[4] and as host materials for nanochemical applications.[5] Although to date the vast majority of compounds have been derived from main group elements such as silicon and aluminum,[2] over recent years there has been increasing interest in incorporating transition metals within three-dimensional and layered framework structures.[6] Such materials have the potential of combining the shape selectivity demonstrated by framework materials with the catalytic, magnetic, optical, and redox properties associated with d-block elements.

However, with the exception of two organically templated uranium(VI) phosphate phases which we recently reported,[7] we are not aware of any syntheses of organically templated materials in which actinide elements such as uranium are incorporated into a layered or microporous framework. We have been interested in the synthesis of these materials for a number of reasons. First, the high coordination numbers and variety of coordination geometries adopted by actinide elements could be expected to result in the formation of new, complex framework architectures when the syntheses are performed in the presence of bulky organic templates. Clearfield and co-workers have demonstrated that in the synthesis of uranyl phosphonates the presence of sterically demanding organic groups on the phosphonate ligands leads to the formation of novel structure types, including porous structures.[8–10] Second, these materials can also be envisioned to exhibit useful catalytic, ion-exchange, and intercalation properties. For example, hydrogen uranyl phosphate (HUP) is a fast hydrogen ion conductor and a versatile ion-exchange reagent,[11–13] and uranium oxide based materials have recently been shown to be effective halocarbon oxidation catalysts.[14] Finally, the existence of a number of stable oxidation states of actinides offers the possibility of synthesizing materials with useful optical and magnetic properties.

The addition of fluoride ions in hydrothermal syntheses has been shown to be a particularly effective method for the synthesis of novel structure types.[15] The fluoride appears to play a role both in aiding the crystallization of the product, and in stabilizing the increased coordination of the metal atoms thus leading to new and more complex framework architectures. We have been exploring the hydrothermal synthesis of new uranium based materials in the presence of both organic templates and fluoride ions, and we report here the synthesis and structural characterization of the first organically templated layered uranium(IV) fluorides to be isolated, namely **1**–**3**.

$(H_3N(CH_2)_3NH_3)U_2F_{10}\cdot 2H_2O$ **1**

$(H_3N(CH_2)_4NH_3)U_2F_{10}\cdot 3H_2O$ **2**

$(H_3N(CH_2)_6NH_3)U_2F_{10}\cdot 2H_2O$ **3**

The fluorides **1**–**3** are synthesized in a one-step process by the reaction of UO_2 under autogenous hydrothermal conditions at 180 °C in the presence of aqueous orthophosphoric acid, aqueous hydrofluoric acid, and the organic structure-directing agent. The materials are isolated as phase pure rhomboid-shaped single crystals in high yield (ca. 70% based

[*] Dr. D. O'Hare, Dr. R. J. Francis, Dr. P. S. Halasyamani
Inorganic Chemistry Laboratory
University of Oxford
South Parks Road, Oxford, OX1 3QR (UK)
Fax: (+44) 1865-272690
E-mail: dermot.ohare@icl.ox.ac.uk

[**] This work was supported by British Nuclear Fuels Limited, the Leverhulme Fund (R.J.F.), and EPSRC. P.S.H. would like to thank Christ Church, Oxford, for a Junior Research Fellowship.

  1433-7851/98/3716-2214 $ 17.50+.50/0